A Pull-Type Taro Harvester Based on the Reverse Locking Capability of the Heart Valve Structure

Yida Qi*, Liang Yu, Lei Hou, Minghe Liu and Kehao Guan

Hohai University, Changzhou, Jiangsu, 213200, China
*Corresponding author's e-mail: 2113673290@qq.com

Abstract. Given the problem that taro harvesting mainly relies on manual harvesting and the mechanization level is low, a taro harvester that can be used in the medium-heavy clay area is proposed. Innovative designs include a valve-like taro supporter to prevent the taro from falling over through reverse locking, a hinge-type limit cutting device to ensure the cutting position is always at the connection between the fruit and the petiole, and a track-type taro feeder wheel that accurately feeds the petiole into the pulling system. Additionally, a soil loosening mechanism, pulling system, and collection device are designed. The length of the arm of the support device is 173mm, the length of the connecting rod is 122 mm, and the spring constant is 300N/m. The shovel length of the soil loosening excavation mechanism is 110mm, and the shovel width is 150mm. It is clear that the main structure of the digging shovel is a direct structure, and the inclination angle of the shovel surface is between 14° and 25°. The handle is adjustable from 150mm to 350mm. At the same time, finite element analysis is conducted on the shovel blade using SolidWorks software to ensure the shovel blade has the appropriate strength through the comprehensive analysis of the track-type feeder wheel, limit cutting mechanism, and drawing mechanism. The drawing speed is between 0.78-1.56m/s. It is determined that the most suitable angle for the pulling system is 40°, and the Adams simulation proves that the system's design is reasonable.

Keywords: A taro harvester; valve-like; track flail wheel; position-limiting cutter

1 Introduction

In China, taro cultivation has a long history and a wide range of cultivation[1]. However, there are many challenges in the harvesting. Taro is cultivated throughout various regions of China [2], but for a long time, our country's main form of taro harvesting has relied on manual or semi-mechanized harvesting [3]. With the continuous improvement of the national standard of living, the market demand for taro continuously increases, and the planting area also increases yearly [4]. Therefore, how to improve the degree of mechanization in taro harvesting has become an urgent problem that needs to be solved.

In the practical application of harvesting machinery, some places directly use potatoes for harvesting. The tuber harvesters that China has successfully developed are

mainly divided into general-purpose and special-purpose types [5]. However, these models are mainly suitable for the sandy soil. Due to the nature of the shear stress of clay soil increasing with the increase of shear displacement [6], the effect of this machine on a heavy clay soil environment is not good. The pulling-type taro harvester studied by Qin Zhanqiang of Jilin Agricultural University [7] and the vibration shovel-type harvester studied by Wang Hongbo of Huazhong Agricultural University [8], although they have made certain innovative designs for the heavy clay soil situation, still face the problem of overcoming the stem falling during the loose soil process. Given the backward situation of mechanized taro harvesting, it is urgent to study a taro harvester suitable for various types of soil operations. Therefore, this paper designs a taro harvester suitable for harvesting taro in medium and heavy clay soil environments, which can provide a new type of machine for taro harvesting.

2 Overall Structure and Working Process

2.1 Overall Structure

The taro harvester is designed to harvest taro by pulling it up. This paper designs a valve-like supporting device to prevent the taro from falling over during harvesting. A hinge-type position-limiting cutter is designed to achieve accurate cutting at the connection between the taro fruit and the stem. A track-type raking device is designed to facilitate the entry of the taro into the pulling system. This device uses friction to allow the taro stalk to enter the pulling system. The pulling system ensures that the taro can be pulled out after the loosening mechanism has pre-loosened the soil. The loosening mechanism pre-loosens the soil around the taro through the coordinated action of the rotating brush and the shovel, reducing the pulling resistance and protecting the integrity of the taro fruit. The overall structure is shown in Figure 1 below.

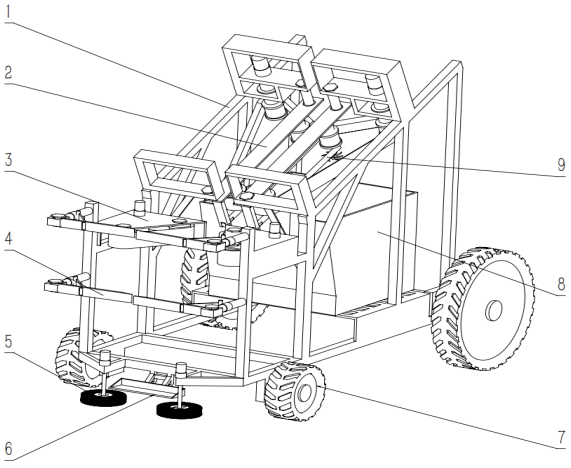

Fig. 1. Overall structure diagram.

Here, the first is rack, the second is the pulling mechanism, the third is track-type feeder wheel, the fourth is a valve-like supporting mechanism, the fifth and the sixth are soil loosening mechanisms, the seventh is wheel assembly, the eighth is collection bin, and the ninth is the hinge-type position-limiting cutter.

2.2 Working Process

After the taro harvester is activated, it moves forward along the harvesting route. Upon reaching the location of the taro, the leaf stalks enter the valve-like supporting device. The supporting device locks the leaf stalks inside the machine through an automatic spring reset function. Then, the copper wire brush is activated to perform soil loosening work. The digging shovel breaks the soil and lifts the entire taro while moving forward. The track-type taro feeder wheel adjusts the leaf stalks, guiding them into the pulling system through friction. The pulling system continues transporting the leaf stalks to the device's rear. During the transportation process, the taro pushes the hinge-type position-limiting cutter upwards. When it reaches a designated position, the cutting device on the position-limiting cutter cuts the connection between the taro and the leaf stalk. After the separation, the leaf stalk is carried outside the device, while the taro is transported to the collection device.

2.3 Technical Parameters

Based on the taro harvester's simulation results, the taro's actual planting conditions, and the parameters of other related models [9-14], the main technical parameters of the entire machine are shown in Table 1 below.

Table 1. Main parameters of taro harvester.

Parameters	Value
Dimensions (L×W×H) /(mm×mm×mm)	1332×652×1255
Velocity /(m·s^{-1})	0.5~1
Working width /mm	600
Power /kW	4.5~5
Working lines	1
Digging depth /mm	105~250

3 Key Component Design

3.1 Valve-Like Supporting Mechanism

The supporting arm incorporates a spring and crank-slider mechanism to perform a function akin to that of a heart valve, as depicted in Figure 2(a). Once the leaf stalk enters the inlet, the mechanism resets and achieves reverse locking under the influence

of the spring, ensuring that the leaf stalk cannot fall out. Subsequently, the leaf stalk is conveyed to the pulling mechanism by the track-type feeder wheel.

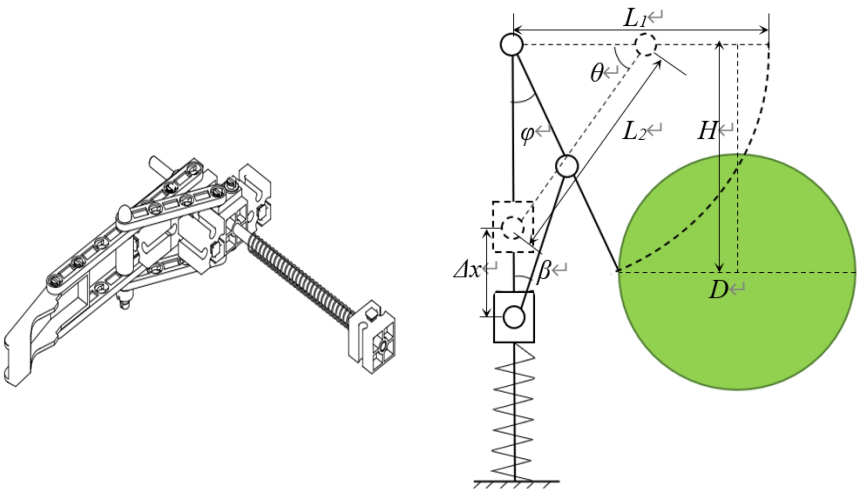

(a) (b)

Fig. 2. Valve-like supporting mechanism.

Figure 2(b) is a schematic diagram for parameter calculation, from which the formula is derived:

$$L_1 = \frac{H}{sin(90° - \varphi)} \tag{1}$$

$$L_2 = L_1 * \frac{\sqrt{2}}{2} \tag{2}$$

$$\Delta x = \frac{L_1}{2} * cos\,\varphi + L_2 * cos\,\beta - L_2 * si\,n\,\theta \tag{3}$$

$$cos\beta = \sqrt{1 - sin\beta^2} = \sqrt{1 - (\frac{L_1}{2 * L_2} * sin\varphi)^2} \tag{4}$$

L_1 — The length of the arm of the support device;
L^2 — The length of the connecting rod;
Δx —The compression length of the spring;
θ — The initial angle between L_1 and L_2;
φ — The angle between L_1 and the frame when the device is about to reset ;
β — The angle between L_2 and the frame when the device is about to reset ;
D — The diameter of the taro leaf stalk;

H — The vertical distance from the center of the leaf stalk to the initial position of the arm of the support device.

Based on the study of taro plants, the average diameter D of the leaf stalk is 250mm [15]. The support device must complete the locking before the soil loosening mechanism starts soil loosening, so H must be less than 200mm (the horizontal distance between the two mechanisms). Therefore, H is set to 150mm. For the stability of the mechanism and the physical model test, the angle φ should not be too small. Otherwise, the angular momentum during the rebound will affect the stability. Therefore, φ is taken as 30°. When θ is 45°, the compression and rebound processes are the most smooth.

In summary, it can be calculated that L_1 = 173mm, L_2 = 122mm, and Δx = 83mm.

After obtaining the value of Δx, the spring constant k can be calculated. The formula is as follows:

$$F = k * \Delta x \tag{5}$$

According to Table 2, the average pulling force required to pull up taro after loosening the soil is 169.47 N. However, in this paper, the crop support device comes into contact and allows the leaf stalk to pass through before the soil is loosened, requiring a pulling force higher than that after loosening. Therefore, the minimum pulling force is selected as a reference for the spring constant. Since we have two springs and assume they have the same spring constant, the force on each spring will be half of the total force.

Table 2. Taro pull-out force after loosening the soil.

Project	Maximum /N	Minimum /N	Average value /N	Standard deviation
Pull-out force	203.13	137.74	169.47	24.83

Assuming the minimum reaction force is 137.74N, the force exerted on each spring is $68.87N$. So the kmax =829.75 N/m. Considering the rebound effect during use, the value of k chooses 300 N/m.

3.2 Soil Loosening and Excavation Mechanism

The soil loosening and excavation mechanism consists of copper wire brushes and excavation shovels.

(1) The copper wire brush is used for soil loosening before the shovel, effectively reducing the resistance of the soil to the shovel's operation and allowing the shovel to cut into the soil more smoothly.

As shown in Figure 3(a), the white bud taro's fruit depth is 200mm, and the thickness is 50mm. Therefore, a brush with a 50-60mm thickness is selected so the bristles can fully cover the taro fruit. It is also known that one side of the taro is 175mm away from the ridge edge. To improve the efficiency of soil loosening and reduce the impact on the fruit, a brush with a 160-180mm diameter is preferable. In summary, we choose a copper wire brush with a thickness of 50mm and a diameter of 180mm, which can

reduce the resistance for the digging shovel by 82.49% and still maintain efficient soil loosening performance even in relatively hard soil.

(2) This excavation shovel is mainly composed of flat surfaces, and its core parameters include shovel length D, shovel width L, shovel face inclination angle θ, shovel face height $h1$, shovel handle height $h2$, and the angle between the shovel face and handle δ, as shown in Figure 3(b).

According to the research on the excavation shovel for the harvesting of tuber crops, the shovel face inclination angle is generally between 14° and 25°, and the friction angle of the soil to rigid materials is between 22° and 45°. Taking the xOy plane as the soil plane, the maximum inclination angle θ of the excavation shovel during operation should, in principle, be less than the friction angle of the object on the shovel face to the shovel. Therefore, after comprehensive consideration, the shovel face inclination angle is taken as 20°.

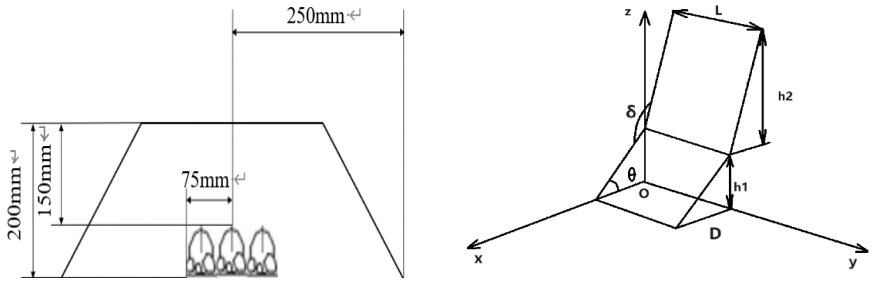

(a) (b)

Fig. 3. Taro planting diagram and shovel calculation diagram.

Taking the white sprout taro as an example, the planting ridge for the taro is 500 millimeters wide, the ridge is 150 millimeters high, and the spacing between plants is approximately 300 millimeters. The depth of the mature fruit is 200 millimeters. Considering that the fruits of the taro usually grow in clusters, with multiple fruits on a single plant with a total diameter ranging from 75 to 150 millimeters, to include all the fruits and to ensure that only one taro plant is excavated at a time, the shovel width L is set to 150 millimeters, and the shovel length D is set to 110 millimeters.

From Figure 1, it can be seen that there is the following relationship between the shovel face height $h1$, the shovel length D, and the shovel face inclination angle θ:

$$h1 = D * tan\theta \tag{6}$$

The design principle of the shovel handle height $h2$ is adjustable to cope with the differences in ridge height and taro depth in different regions. At the same time, different shovel handle lengths can be used to consider the degree of connection of the taro. This machine can achieve an adjustable range of the shovel handle from 150mm to 350mm.

We perform a mechanical analysis of the shovel blade, and the formula is shown in Equation (3).

$$F_q = F_p + f \tag{7}$$

$$F_p = SL'\rho g tan(\lambda + \xi) \tag{8}$$

Fq-- Traction force required for the device to work normally in Newtons (N);
F_p-- Force required for the excavation shovel to cut through the soil in Newtons (N);
f-- Soil adhesion force in Newtons (N).
$F_q = 2373.63N$ is imported into SolidWorks for finite element analysis.

The stress analysis results are shown in the following Figure 4. According to the third strength theory, the shovel and the parts connected to the main body meet the stress requirements, and there is no situation where the stress exceeds the maximum that the structure can withstand.

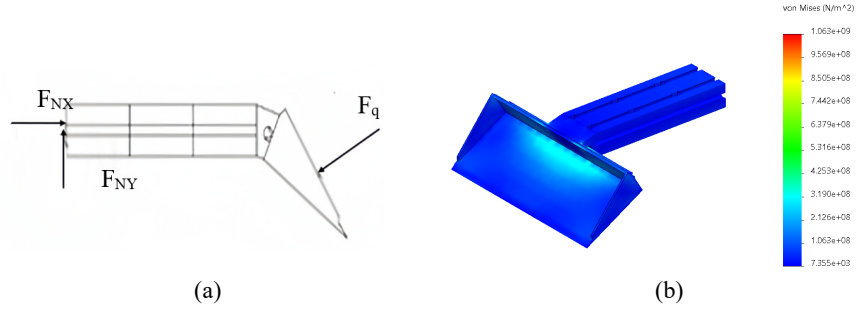

(a) (b)

Fig. 4. Finite element analysis diagram of a blade.

Figures 4 (a)(b) are force and stress finite element analyses. The strain and displacement analysis results show that the part most prone to deformation is the front end of the shovel blade because the front end is the thinnest and comes into contact with the soil first. Digging into sandy loam soil should be easier than ordinary soil so the deformation situation will be better than the software analysis.

3.3 Track-Type Taro Feeder Wheel

The mechanism adopts a track-type pulley, as shown in Figure 5. The wheel can evenly distribute power through chain transmission, ensuring continuity and stability. By utilizing the friction force of the timing belt, the track can guide the leaf stalk into the pulling system. This helps to ensure the stable feeding of the leaf stalk and can prevent it from swaying during the harvesting process, thereby improving the accuracy of the harvest. The speed of the wheel's timing belt is consistent with the speed of the pulling system's timing belt.

The weeding wheel is mainly composed of gears and tracks, and its core parameters include the weeding angle θ, gear longitudinal spacing h1, h2, gear width spacing l1, l2, and the spacing between the weeding wheels D (h1 = h2, l1 = l2). Considering that the diameter of a single taro leaf stalk is about 50mm and the number of leaf stalks per plant is around 3-5, the machine is designed with D = 120mm and θ = 45°, ensuring that leaf stalks of different sizes can enter the subsequent mechanism while preventing

the leaf stalks from falling over due to excessive spacing between the weeding wheels. Let the total length of the gear be $H = h_1 + h_2$, and the total width $L = l_1 + l_2$, then as long as H, L > D is ensured. To allow time for the weeding wheel to correct the taro leaf stalks, the actual total length and width should be greater than D. Experimental measurements indicate that the general correction time for the leaf stalks is about 2 seconds, and n = 75 r/min, combined with the gear diameter d = 5cm:

$$H = h1 + h2 = 2 * \pi * d * (n/60) * sin\theta \tag{9}$$

$$L = l1 + l2 = 2 * \pi * d * (n/60) * cos\theta \tag{10}$$

By substituting the data, we get that $H = L = 277.4975$mm under normal circumstances. Therefore, the machine is designed with $H = L = 300$mm.

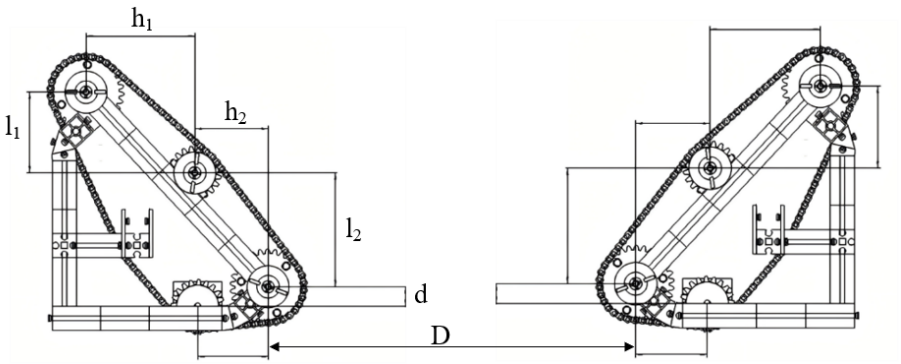

Fig. 5. Track-type taro feeder wheel.

Compared to the traditional mechanism [16] which is illustrated in Figure 6, the track-type taro feeder wheel mechanism reduces the breaking of leaf stalks during the process, protecting the integrity of the crops. This design is beneficial as it minimizes crop damage, which can be particularly important for maintaining the quality and yield of the harvest.

Fig. 6. Traditional taro feeder wheel.

Due to the design and operation of the track-type taro feeder wheel, the possibility of leaf stalks getting stuck during the harvesting process is reduced, which in turn lowers the risk of mechanical faults, minimizing damage to the leaf stalks and reducing blockages.

3.4 Position Limiting Cutter

The position-limiting cutting machine mainly consists of the following key components: hinge, cutting device, and strip-shaped fixing device.

It is articulated on two hinges and made of Q235 steel. According to the data, the diameter of a single taro leaf stalk is between 3-5 cm, and a single taro plant consists of 5-6 leaf stalks. Therefore, the spacing of the two strip-shaped devices is set at 250 mm. As the taro fruit rises during the transmission process, it will drive the ascent of the fixing device, ensuring that the cutting position is always at the connection point between the fruit and the leaf stalk. Once it reaches the designated position, the cutting device cuts the connection between the taro and the leaf stalk, separating the taro from the leaf stalk. The actual object diagram is as shown in Figure 7.

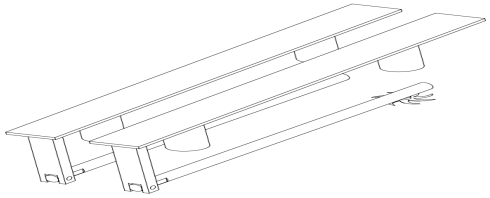

Fig. 7. Position limiting cutter.

3.5 Pulling System

The pulling effect is influenced by the opening angle of the pulling belt, as shown in Figure 8 below. The pulling belt exerts a force on the stem that converges, lifts, and pushes over the stem. The combined force can be orthogonally decomposed into horizontal and vertical components *Tx* and *Ty*.

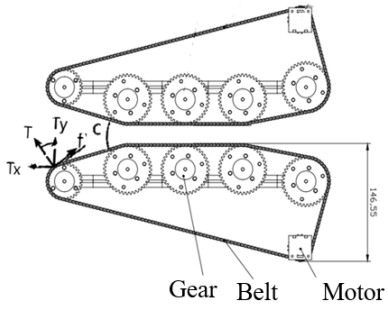

Fig. 8. The Belt exerts a force on the stem.

$$T_x = T * \sin\frac{c}{2} \tag{11}$$

$$T_y = T * \cos\frac{c}{2} \tag{12}$$

T— The combined force exerted by the pulling belt on the stem.
C— The opening angle of the two sides of the synchronous belt.

From Equation (11), it can be deduced that the opening angle C is proportional to the force that pushes and topples the plant. However, the smaller the opening angle C, the closer the pulling belt is to the ridge surface, which requires a higher degree of flatness in the field and increases the gathering time, potentially affecting the pulling effect. Therefore, an opening angle of C=120° is most suitable.

The spacing between the pulling belts is related to the thickness of the stem; if it is too large or too small, a gap can affect the pulling effect. According to reliable data, a spacing y of 25 mm and a clamping point height L1 of 120 mm are optimal. Additionally, to ensure the pulling system can capture thinner leaf stalks, the machine is equipped with tensioning devices on both sides of the pulling system, which apply pressure to leaf stalks of varying thicknesses to ensure they do not slip when in contact with the synchronous belt, thus preventing the inability to pull up the taro.

4 Simulation Analysis

The stem should be pulled to ensure the success rate of stem pulling and minimize the pulling force vertically upwards. The absolute pulling speed is influenced by the machine's forward speed, the pulling belt speed, and the installation angle of the pulling device [17], as shown in Figure 9 below.

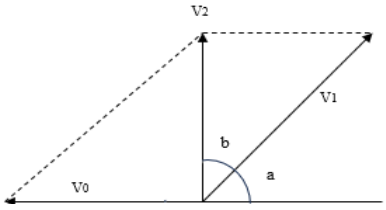

Fig. 9. Motion synthesis.

$$F = \frac{v_1}{v_2} = \frac{\sin(a+b)}{\sin b} = \frac{1}{\cos a} \tag{13}$$

$$a + b = 90° \tag{14}$$

F— Pulling speed ratio;
a — Installation inclination;
V_0— Machine forward speed, in meters per second (m/s);
V_1— Pulling belt speed, in meters per second (m/s);
V_2— Absolute speed at the pulling point, in meters per second (m/s).

From Equation (13), it can be seen that the pulling belt speed is directly proportional to the installation angle. That is, the smaller the pulling belt speed, the smaller the installation angle. Under the condition of conveying to the same height, the overall machine becomes longer. Therefore, we check the information to find out that F=1.3 is the best. From this, it is known that when cos a = 0.76, that is, a = 40°, it is the most suitable. The pulling belt speed ranges between 0.78-1.56 m/s.

The different installation angles lead to different directions of frictional force on the taro petiole, thereby affecting the pulling of the taro, especially its horizontal displacement. If the horizontal displacement is too large, it will cause the petiole to slip off. In order to determine the optimal installation angle, this paper uses ADAMS for simulation. Since the synchronous belt primarily provides static friction to pull the taro, we simulate the static friction of the pulling system by applying forces to the taro leaf stalk at angles of 20°, 30°, 40°, and 50° with the horizontal plane. The horizontal displacement of the lowest point of the taro is measured, as shown in Figure 10 below.

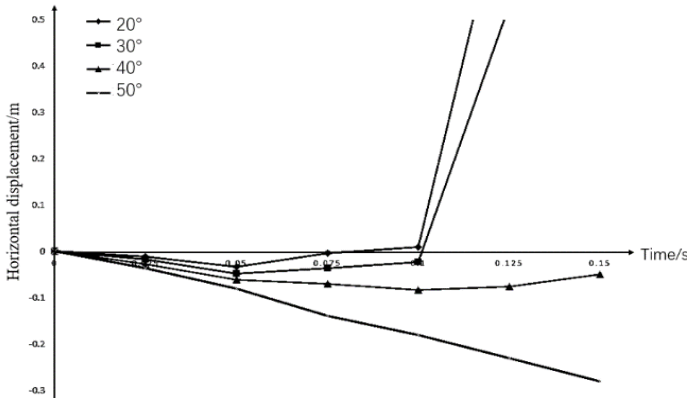

(a) (0-0.15s)

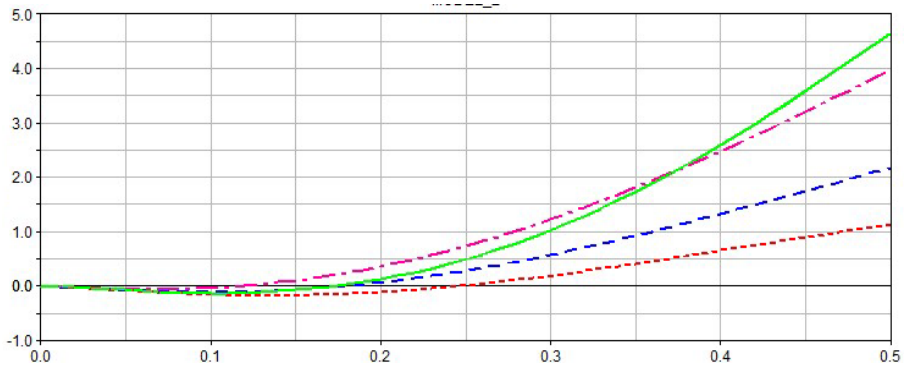

(b) (0-0.5s)

Fig. 10. Horizontal displacement of taro at different inclination angles of the drawing system.

From Figure 10, it can be seen that as the installation angle increases, the displacement of the taro along the negative half-axis increases within 0-0.15 seconds, but the displacement along the positive half-axis decreases within 0-0.5 seconds. The negative half-axis displacement is the swing amplitude of the taro during the pulling operation. To ensure the pulling operation is stable, the swing amplitude should not be too large; otherwise, the petioles will be prone to falling off. The displacement along the positive half-axis is related to the length of the machine's body. Considering the machine's cost and movement, the body length should not be too long; otherwise, it not only increases the cost, but the motor power may not be sufficient. Combining the information from the two charts above, it is known that although the swing amplitude is not large at 20° and 30°, the positive displacement within 0.5 seconds is too large, which greatly increases the cost. At 50°, the swing amplitude is too large, causing the petioles to fall off easily. However, at 40°, the taro's swing amplitude is not large, and the positive displacement is moderate, which aligns with the optimal calculation results.

5 Conclusions

This article proposes a taro harvester suitable for most taro harvesting environments, taking the white sprout taro as the main research object. The overall dimensions of the machine are designed to be 1332×652×1255 (length × width × height). Innovative designs include a valve-like taro supporter to prevent the taro from falling over through reverse locking, a hinge-type limit cutting device to ensure the cutting position is always at the connection between the fruit and the petiole, and a track-type taro feeder wheel that accurately feeds the petiole into the pulling system. Additionally, a soil loosening mechanism, pulling system, and collection device are designed. The ADAMS software is utilized to study the horizontal displacement of the taro petiole at different inclinations of the pulling system to verify whether the theoretically derived 40° inclination is suitable. The results indicate that the pulling system's design requirements are met at a 40° angle.

References

1. Wei Wu, Qingtao Chang, An Wang. Research Progress on Chinese Taro Germplasm Resources [J]. Anhui Agricultural Sciences, 2021, 49(14): 4-7.
2. Juxian Guo, Yan Yin, Kang Tang, et al. Research Progress and Prospects on Taro Germplasm Resources [J]. Guangdong Agricultural Sciences, 2021, 48(09): 81-90.
3. Mengyue Zhang. 2021. Design and Test of Taro Harvester [M]. Master's Thesis, Huazhong Agricultural University, https://link.cnki.net/doi/10.27158/d.cnki.ghznu.2021.000562.
4. Zhanqiang Qin. 2020. Design and Research of Red Sprout Taro Harvester [M]. Master's Thesis, Jiangxi Agricultural University, https://link.cnki.net/doi/10.27177/d.cnki.gjxnu.2020.000087.
5. Shiwen Ma, Guihong Huang. Research and Application of Dual Drive Potato Harvester [J]. Agricultural Machinery Quality and Supervision, 2017 (10): 24-25.

6. Tingting Sun, Yu Chen, Xianze Shi, et al. Study on the Mechanical Properties of Different Clays Based on Direct Shear Test [J]. Journal of Yancheng Institute of Technology (Natural Science Edition), 2024, 37(01): 31-36.
7. Hongbo Wang. 2022. Design and experiment of vibration shovel digging clamp type taro excavator [D]. Huazhong University of Science and Technology, https://link.cnki.net/doi/10.27158/ d.cnki.ghz nu.2022.001124.
8. Zhanqiang Qin, Renxin Liu, Licai Chen, Yifan Zeng, Xiuwen He. Design and simulation analysis of taro harvester. China Agricultural Machinery Chemistry Report,2020,41(1):31-36.
9. Jian Liao, Rui Wang, Xu Li, et al. Design and Experimental Study of Taro Harvester [J]. Hubei Agricultural Mechanization,2017(01):63-64.
10. Peitong Zhang, Hongru Xiao, An Wang, et al. New agricultural machinery and its key points for light and simple cultivation of taro [J]. Yangtze River vegetables food,2017(15):11- 13.
11. Smith, J. & Johnson, K. The EVO-280 Potato Harvester: A Comprehensive Review [J]. Journal of Agricultural Machinery, 2019, 45(3): 56-63.
12. Takahashi, M. & Suzuki, Y. AVR Series Harvester: Efficiency and Reliability Analysis [J]. Journal of Farm Machinery, 2020, 67(1): 12-21.
13. Davis, R. & Brown, T. Autonomous Navigation and Precision Harvesting of Taro Using LiDAR and GPS [J]. International Journal of Agricultural and Biological Engineering, 2021, 14(3): 1-9.
14. Wang, Q.&Liu, P. Application of Deep Learning in Taro Recognition and Localization for Autonomous Harvesting [J]. Agricultural Engineering International: CIGR Journal, 2023, 25(1): 1-12.
15. Xiang Ju. High yield planting technology of "Bai Yu No.1" taro in Changle County, Shandong Province. Northern horticulture,2015(20):54-55.
16. Fuping He, Zhi Chen, Zirui Zhang, Zengde Han, Bangxing Gan, Xiaodong Qiao. Design and Experiment of a Wheel Type Corn Harvesting Platform for Cropping [J]. Journal of Agricultural Machinery,2014,45(06):112- 117.
17. Jialin Hou, Yanyu Chen, Yuhua Li, et al. Development of a self-propelled onion combine harvester with quantitative placement [J]. Journal of Agricultural Engineering, 2020, 36(07): 22-33.